

A Broad Spectrum Inhibitor of Influenza A and B Viruses Targeting the Viral Nucleoprotein

Kris M White, Pablo Abreu, Hui Wang, Paul D De Jesus, Balaji Manicassamy, Adolfo García-Sastre, Sumit K Chanda, Robert J DeVita, and Megan L. Shaw

ACS Infect. Dis., **Just Accepted Manuscript** • DOI: 10.1021/acsinfecdis.7b00120 • Publication Date (Web): 21 Dec 2017

Downloaded from <http://pubs.acs.org> on December 26, 2017

Just Accepted

“Just Accepted” manuscripts have been peer-reviewed and accepted for publication. They are posted online prior to technical editing, formatting for publication and author proofing. The American Chemical Society provides “Just Accepted” as a free service to the research community to expedite the dissemination of scientific material as soon as possible after acceptance. “Just Accepted” manuscripts appear in full in PDF format accompanied by an HTML abstract. “Just Accepted” manuscripts have been fully peer reviewed, but should not be considered the official version of record. They are accessible to all readers and citable by the Digital Object Identifier (DOI®). “Just Accepted” is an optional service offered to authors. Therefore, the “Just Accepted” Web site may not include all articles that will be published in the journal. After a manuscript is technically edited and formatted, it will be removed from the “Just Accepted” Web site and published as an ASAP article. Note that technical editing may introduce minor changes to the manuscript text and/or graphics which could affect content, and all legal disclaimers and ethical guidelines that apply to the journal pertain. ACS cannot be held responsible for errors or consequences arising from the use of information contained in these “Just Accepted” manuscripts.

1
2
3 **A Broad Spectrum Inhibitor of Influenza A and B Viruses Targeting the Viral**
4
5 **Nucleoprotein**
6
7
8
9

10 Kris M. White¹, Pablo Abreu Jr.¹, Hui Wang^{2^}, Paul D. De Jesus³, Balaji Manicassamy^{1#},
11
12 Adolfo García-Sastre^{1,4,5}, Sumit K. Chanda³, Robert J. DeVita^{2,6} and Megan L. Shaw^{1*}
13
14

15
16
17 ¹Department of Microbiology, ²Department of Pharmacological Sciences, ³Immunity and
18
19 Pathogenesis Program, Infectious and Inflammatory Disease Center, Sanford Burnham
20
21 Prebys Medical Discovery Institute, 10901 North Torrey Pines Road, La Jolla, California
22
23 92037, USA, ⁴Department of Medicine, Division of Infectious Diseases, ⁵Global Health
24
25 and Emerging Pathogens Institute, ⁶Drug Discovery Institute, Icahn School of Medicine
26
27 at Mount Sinai, New York, NY 10029, USA,
28
29
30

31
32
33 [^]Present Address: Suzhou Novartis Pharma Technology Co., Ltd. 18 Tonglian Road,
34
35 Riverside Industrial Park, Changshu Economic Development Zone, Changshu / Jiangsu
36
37 Province 215537, China.
38

39
40 [#]Present Address: Department of Microbiology, University of Chicago, Chicago, Illinois,
41
42 USA.
43

44
45 *Corresponding author

46
47 Department of Microbiology
48
49 Icahn School of Medicine at Mount Sinai
50
51 One Gustave L. Levy Place
52
53 New York, NY 10029, USA.
54
55

1
2
3 Tel.: +1-212-241-8931
4

5 megan.shaw@mssm.edu
6
7
8
9
10
11

12 S119 was a top hit from an ultra-high through-put screen performed to identify novel
13 inhibitors of influenza virus replication. It showed a potent antiviral effect ($IC_{50} = 20$ nM)
14 and no detectable cytotoxicity ($CC_{50} > 500$ μ M) to yield a selectivity index greater than
15 25,000. Upon investigation, we found that S119 selected for resistant viruses carrying
16 mutations in the viral nucleoprotein (NP). These resistance mutations highlight a likely
17 S119 binding site overlapping with, but not identical to that found for the compound
18 nucleozin. Mechanism of action studies revealed that S119 affects both the
19 oligomerization state and cellular localization of the NP protein which impacts on viral
20 transcription, replication and protein expression. Through a hit-to-lead structure-activity
21 relationship (SAR) study, we found an analog of S119, named S119-8, which had
22 increased breadth of inhibition against influenza A and B viruses accompanied by only a
23 small loss in potency. Finally, in vitro viral inhibition assays showed a synergistic
24 relationship between S119-8 and oseltamivir when they were combined, indicating the
25 potential for future drug cocktails.
26
27
28
29
30
31
32
33
34
35
36
37
38
39
40
41
42
43
44
45
46

47 Key Words: influenza, antiviral, nucleoprotein, aggregation, nucleozin
48
49
50
51
52
53
54
55
56
57
58
59
60

1
2
3 Influenza virus is an important human pathogen, which accounts for significant morbidity
4 and mortality worldwide in annual epidemics. In addition, through genomic reassortment,
5
6
7 influenza A virus has and will continue to cause periodic global pandemics. The worst of
8
9
10 these was the 1918 “Spanish flu”, which caused an estimated 50-100 million deaths.³²

11
12 During the most recent H1N1 pandemic in 2009, efforts to produce and deliver a vaccine
13
14
15 to protect the world population were outpaced by the spread of the virus. This failure of
16
17 the influenza pandemic vaccination program highlights the importance of antiviral
18
19 therapies under pandemic conditions. Moreover, coverage of seasonal influenza vaccines
20
21 is estimated at only 33-73%³³, leaving a significant proportion of the population
22
23
24 vulnerable to infection every year.

25
26
27
28 There is an urgent need for new antiviral therapies against influenza virus, as the two
29
30
31 current FDA-approved drug classes have both suffered from significant issues of viral
32
33
34 resistance, either currently or in the recent past. The CDC no longer recommends the M2
35
36 inhibitors (amantadine and rimantadine) for use in the clinic due to high levels of
37
38 resistance in both H1N1 and H3N2 circulating strains¹. Neuraminidase inhibitors, of
39
40 which the orally available oseltamivir is the most heavily prescribed, are currently the
41
42 only FDA approved antiviral drugs recommended for use against influenza virus.

43
44 Although oseltamivir resistance remains relatively low (0-0.8%) currently, during the
45
46
47 2007-2008 influenza season the circulating H1N1 strain gained nearly complete
48
49
50 resistance². This oseltamivir resistant strain was fortunately replaced by the 2009 H1N1
51
52
53 pandemic strain, but the quick spread of this resistance, to our last line of antiviral

1
2
3 defense, is highly concerning and highlights the necessity of finding new therapeutics
4
5 with different targets.
6
7
8
9

10 The influenza nucleoprotein (NP) is a critical factor in many stages of the viral life cycle.
11
12 The NP protein coats the viral genomic RNA to form ribonucleoproteins (RNPs)³ and is
13
14 involved in transportation of RNPs to the nucleus⁴, viral transcription and replication^{5,6},
15
16 and virion assembly⁷. Therefore, NP is localized within the cytoplasm during viral entry,
17
18 the nucleus during viral replication and finally in the cytoplasm again during egress⁸.

19
20 Knowledge of the NP crystal structure²⁰ and RNP cryo-EM structure^{3,9} has significantly
21
22 advanced our understanding of the multimeric nature of NP and how important its
23
24 oligomeric state is to viral replication. Recently, the NP protein was shown to be a valid
25
26 and efficient target for inhibition of influenza virus replication and pathogenesis.^{10,11,12}
27
28
29

30 The compound, nucleozin, was found to inhibit influenza via blocking NP import into the
31
32 nucleus and causing abnormal aggregation within the cytoplasm¹¹.
33
34
35
36

37 In a high through-put screen which we have previously described¹³, 919,960 compounds
38
39 were screened for inhibition of influenza virus replication in a cell-based assay. In this
40
41 screen, we identified a number of influenza specific inhibitors of viral replication with
42
43 sub-micromolar IC₅₀'s. One of these compounds, designated S119, was found to inhibit
44
45 replication through alteration of the oligomeric state of the NP protein. Herein we discuss
46
47 the mechanism of action of S119 and a preliminary structure activity relationship (SAR)
48
49 study to improve the breadth of antiviral activity as proof-of-concept for future drug lead
50
51 optimization.
52
53
54
55
56
57

Results and Discussion

S119 is a Specific Inhibitor of Influenza A Virus. The compound S119 (Figure 1a) was identified as a potent hit from a previously published cell-based screen of nearly one million compounds utilizing a luciferase-based reporter influenza A/WSN/33 H1N1 (WSN) virus¹⁴. S119 potently inhibited both the reporter virus and wild-type WSN virus in MDCK cells with an IC₅₀ of 60 nM (Figure 1b). When tested in the human lung cell line, A549, S119 caused a 4 log reduction in WSN viral titers resulting in an IC₅₀ of 20 nM (Figure 1c). Cytotoxicity of S119 was tested in A549 cells using the CellTiter-Glo system (Promega) and the compound showed very little toxicity at concentrations as high as 500 μM, yielding a minimum SI of 25,000. When examined for activity against other strains of influenza A virus, we found that S119 caused a 77% reduction in the pandemic strain A/California/2009 (H1N1) infectious titer, but was ineffective against A/Puerto Rico/8/1934 (PR8, H1N1), A/Panama/2007/1999 (H3N2) and A/Vietnam/1203/2004 (H5N1) (Table 2).

S119 Inhibits a Post-Entry Step and Targets the NP protein. To begin to dissect the mechanism of action of S119, we first sought to determine at which stage of viral infection the compound was inhibiting. We performed a time of addition assay at an MOI of 1 (A/WSN/33) with S119 treatments at -2, 0, 2, 4, 6, or 8 hours relative to infection. We found that S119 was able to maximally inhibit virus replication when added before infection and up to 2 hours after infection. The compound also showed significant virus inhibition when added 4 hours after infection, while still maintaining a 1 log effect at 6 hours (Figure 2). This indicated that S119 was exerting its effect at a post-entry step of

1
2
3 the viral life cycle, possibly during viral transcription and replication. To determine
4 whether S119 was targeting a viral protein, influenza virus was passaged in the presence
5 of S119 and S119-resistant viruses were selected. Briefly, A549 cells were infected with
6 influenza A/WSN/33 virus at an MOI of 0.01 in the presence of 2 μ M S119, which
7 yielded enough viral progeny for subsequent passages at a low MOI as detected by viral
8 plaque assay. The remaining passages were tracked by hemagglutination assay to
9 determine if the virus had escaped inhibition by S119. Viral resistance to S119 was
10 detected after 3 to 4 passages and isolates were obtained from 7 independent experiments,
11 with 3 viruses plaque purified from each experiment and submitted for full genome
12 sequencing. Of the 21 sequenced viral genomes, 11 contained mutations leading to 7
13 unique amino acid changes all occurring within the nucleoprotein (NP). When these
14 resistance mutations were mapped onto the crystal structure of the NP protein, 6 of the 7
15 residues were found to form a single pocket on the surface of the protein (Figure 3a). The
16 remaining mutated residue, R98 was found to be within close proximity to this pocket as
17 well. We found this particularly illuminating due to the 246 amino acid distance between
18 the most distal residues (Y40 and A286). This indicated to us, that not only was NP the
19 likely target for S119 inhibition, but this pocket highlighted by resistance mutations is
20 also likely the S119 binding site within the NP protein. This putative binding pocket is
21 located in the "body" domain of NP where an important NP-NP interaction occurs in the
22 formation of the ribonucleoprotein (RNP) complex. Quite interestingly, a known inhibitor
23 of NP, nucleozin¹¹, has been shown to have two binding sites on either side of the
24 putative S119 binding pocket¹⁵. Nucleozin is proposed to cause an atypical NP-NP
25 interaction through the "body" domains¹², which subsequently leads to formation of
26
27
28
29
30
31
32
33
34
35
36
37
38
39
40
41
42
43
44
45
46
47
48
49
50
51
52
53
54
55
56
57
58
59
60

1
2
3 large, replication deficient NP aggregates. S119 is structurally unrelated to nucleozin and
4
5 the binding sites of the two compounds appear to be distinct with a small amount of
6
7 overlap. Previous publications have shown that mutations at positions Y40, S50, D51,
8
9 and A286 (which confer S119 resistance) do not cause resistance to nucleozin, while a
10
11 mutation at position R55 causes resistance to both compounds¹². The NP protein is highly
12
13 conserved amongst influenza viruses, so it is surprising that S119 did not have a broad
14
15 spectrum of inhibition, particularly in the case of the PR8 strain, which is closely related
16
17 to WSN. The NP proteins of WSN and PR8 share identical amino acids at each of the
18
19 resistance mutation sites identified, indeed these sites are also 99.8 to 100% conserved in
20
21 currently circulating influenza A viruses. Even currently circulating influenza B viruses
22
23 show 100% conservation of identical or similar amino acids in the corresponding sites of
24
25 the influenza B NP protein. Interestingly, there is a proline at position 283 of the PR8 NP
26
27 protein, whereas there is a serine at this position in WSN. This S283P substitution would
28
29 have a significant effect on the structure of the alpha-helix in which the A286 resistance
30
31 site resides and therefore change the conformation of the putative S119 binding pocket. It
32
33 may be that the extended structure of the S119 molecule is highly intolerant of any
34
35 change to the size of its binding pocket.
36
37
38
39
40
41
42
43

44 To further explore the impact of resistance to S119, the Y40F mutation was introduced
45
46 into a recombinant influenza A/WSN/33 virus using a reverse genetics system¹⁶. This
47
48 virus, referred to as rWSN-Y40F, was not impaired for growth when compared to a wild
49
50 type recombinant virus in a multi-cycle growth assay (data not shown). When S119 was
51
52 tested for efficacy against rWSN-Y40F, the mutant virus had a resistant phenotype, with
53
54
55
56
57
58
59
60

1
2
3 an IC_{50} 50-fold higher than the wild type counterpart (Figure 3b). Conversely, the IC_{50} for
4
5 nucleozin was only 4.5-fold higher with the Y40F NP mutation (Figure 3c). This minor
6
7 resistance phenotype is in agreement with the literature that this residue is adjacent to, but
8
9 not part of, the nucleozin binding site in NP.¹²
10
11
12
13

14 **S119 Causes Aggregation of the NP protein.** The importance of the oligomeric state of
15
16 the influenza virus NP protein has been well defined through previous biochemical and
17
18 structural studies^{17, 18, 19}, and the location of the S119 resistance mutations near to those
19
20 conferring nucleozin resistance indicated that alteration of the NP-NP interaction at this
21
22 interface may be the mechanism of S119 antiviral activity. To determine whether S119
23
24 has an effect on NP oligomeric state, purified baculovirus-expressed NP was incubated
25
26 with and without compound for 30 minutes in the presence or absence of purified viral
27
28 RNA and analyzed by blue native PAGE. In the absence of RNA, the purified NP runs at
29
30 a low molecular weight, likely representing monomeric NP (Figure 4a, upper panel). The
31
32 band appears as a doublet because of a slightly truncated form of NP being co-expressed
33
34 with the full-length protein during baculovirus expression. This was confirmed via
35
36 western blot analysis, where the truncated band is recognized by both anti-NP and anti-
37
38 His antibodies. This indicated a C-terminally truncated NP species, because the His-tag is
39
40 located on the N-terminus of the recombinant protein. In Figure 4a (lower panel, lane 1),
41
42 both forms of NP are shown to be capable of oligomerizing on RNA and therefore the
43
44 truncated protein should not affect the experimental outcome. An active analog of the
45
46 published PB2 inhibitor VX-787²⁰ was used as a negative control. When treated with
47
48 S119 or nucleozin in the absence of RNA, the low molecular weight NP band is lost
49
50
51
52
53
54
55
56
57
58
59
60

1
2
3 relative to controls. For nucleozin, it has been described that NP shifts into an
4 unresolvable higher order complex¹¹, and this is likely the case for S119 treatment as
5 well. Interestingly, S119 appears to have a greater effect on the low molecular weight NP
6 than nucleozin at the same concentration, despite nucleozin having similar potency in
7 viral inhibition assays. In the presence of influenza vRNA, most of the NP runs at a
8 higher molecular weight (indicative of oligomers), which are clearly visible in the native
9 PAGE gel, but a small amount of low molecular weight NP remains present. In the case
10 of nucleozin treatment, this oligomer ladder becomes a smear on the gel, indicating the
11 formation of an aggregate. When treated with S119, a faint oligomer ladder still remains
12 and the low molecular weight band is completely lost. Our interpretation of this effect is
13 that S119 perturbs the NP oligomerization state both in the presence and absence of viral
14 RNA, but may be doing so in a manner different from nucleozin. These results could
15 indicate that S119 has a higher affinity for NP in the monomeric state as compared to
16 oligomerized NP within the RNP structure. While these experiments were suggestive of
17 the S119 mechanism of action, the inherent limitations of the *in vitro* system with a
18 tagged protein outside of the context of an influenza virus-infected cell meant that
19 confirmation of these results would be required from alternative experimental systems.
20
21
22
23
24
25
26
27
28
29
30
31
32
33
34
35
36
37
38
39
40
41
42
43

44 Due to the inability to resolve higher order aggregations in the native PAGE system it
45 was difficult to address the exact effect of S119 on NP oligomerization, so size exclusion
46 chromatography was employed to investigate this further. Lysates from WSN infected
47 A549 cells treated with S119 or nucleozin were applied to a Superose6 column and 1 ml
48 fractions were collected. S20, a compound that targets HA¹³, was used as a negative
49
50
51
52
53
54
55
56
57
58
59
60

1
2
3 control. In infected cells, the vast majority of the expressed NP is present in RNP
4
5 complexes, which are quite large and appeared in the exclusion volume (fraction 8) in the
6
7 Superose6 column (Figure S1). However, some of the NP was maintained in a lower
8
9 molecular weight pool, which is likely to be monomers or small oligomers (fractions 17-
10
11 19). A large NP aggregate would be expected to appear in the exclusion fraction similar
12
13 to the RNP structure, making differentiation of these two states difficult in this
14
15 experimental set up. Therefore, lysates were RNase A treated following drug treatment to
16
17 disrupt the RNP complexes prior to being applied to the column for subsequent
18
19 experiments. Once the RNPs were RNase treated, a moderate molecular weight NP
20
21 oligomer pool was observed in fractions 11 through 14. A clear shift to smaller oligomers
22
23 (fractions 14-15) was observed in both S119 and nucleozin treated samples along with a
24
25 distinct loss of the low molecular weight NP pool (Figure 4b). While a reduction in the
26
27 oligomeric size of NP was unexpected, the fact that the known NP aggregator, nucleozin,
28
29 showed a similar effect indicated that S119 could be causing a similar formation of
30
31 abnormal NP complexes. The shift to smaller oligomers might be due to changes in the
32
33 exposure of viral RNA to RNase A in the presence of drug. For example, if the NP
34
35 aggregates caused by both S119 and nucleozin were to make the RNA more accessible to
36
37 enzymatic digestion than the RNA within the tightly packed RNP structure, one would
38
39 expect the observed reduction in oligomer size after RNase A treatment. Interestingly,
40
41 S119 appeared to cause a greater reduction in the low molecular weight NP pool than that
42
43 observed with nucleozin and this effect occurred in the absence of RNase treatment as
44
45 well (Figure S1), which aligns well with our assays using purified NP protein (Figure 4a).
46
47
48
49
50
51
52
53
54 When we examined NP from the rY40F S119-resistant virus, we found that
55
56
57
58
59
60

1
2
3 oligomerization was unaffected by S119 treatment, but was altered by nucleozin similarly
4
5 to wild type virus (Figure 4c).
6
7
8
9

10 Finally, immunofluorescence microscopy was performed on WSN infected A549 cells to
11 determine NP localization at 2, 4, 6 and 24 hours after infection. The incoming NP
12 protein (as part of the RNP) is first found in the cytoplasm during viral entry into the cell.
13
14 Then, at around 4 hours post infection, newly synthesized NP is detected exclusively in
15 the nucleus, and later it is exported to the cytoplasm for packaging into virions. This
16 temporal pattern of NP localization was observed in the DMSO control experiment
17 (Figure 5). With nucleozin treatment, NP remains exclusively in the cytoplasm and
18 begins to form visible aggregates by 4 hours post infection, consistent with previous
19 publications.¹¹ In the case of S119, while NP translocation to the nucleus was delayed, it
20 was not excluded. At 6 hours post infection NP was observed in the nucleus, though with
21 much weaker expression. Aggregation of NP was also observed under S119 treatment,
22 but not until the 24 hour post infection time point (Figure 5). The S119-induced
23 aggregates also appeared to be larger than those from nucleozin, possibly due to an
24 overall higher expression of NP in the presence of S119 compared to nucleozin. All of
25 these data taken together suggest that S119 is causing an abnormal oligomerization of the
26 NP protein, likely resulting in the formation of large aggregates.
27
28
29
30
31
32
33
34
35
36
37
38
39
40
41
42
43
44
45
46
47
48

49 **NP Aggregation by S119 Causes a Segment Specific Inhibition of Viral**

50 **Transcription.** The nucleoprotein is essential for both viral transcription and replication.
51
52 Therefore, we wanted to determine whether S119-induced NP aggregation caused any
53
54
55
56
57
58
59
60

1
2
3 downstream effects on the production of mRNA and vRNA from the various influenza
4 genomic segments. We utilized primer extension assays to analyze mRNA and vRNA
5 production and western blot to detect protein expression from the PB2, NP and NS
6 segments as representatives of long, medium and short segments respectively. Treatment
7 of WT WSN infected A549 cells with nucleozin caused a complete loss of both mRNA,
8 vRNA and viral protein expression from all three segments, regardless of size (Figure 6a,
9 b, c). In contrast, S119 inhibition resulted in a segment specific effect. In the presence of
10 S119, mRNA expression from the PB2 segment was reduced to undetectable levels
11 (Figure 6a), although the small amount of PB2 protein indicates that there is a minimal
12 level of mRNA expression. In the case of the NP segment, mRNA expression was
13 severely reduced by S119, but still observable and NP protein levels were moderately
14 reduced (Figure 6b). Finally, mRNA expression from the NS segment was slightly
15 reduced, but NS1 protein expression was unaffected (Figure 6c). vRNA could not be
16 detected from any segment under S119 treatment, indicating a block in replication. In
17 contrast, the rY40F-WSN virus was completely resistant to S119 inhibition of
18 transcription and replication, while nucleozin exhibited efficient inhibition of this virus
19 (Figure 6d, e, f). The loss of global vRNA expression could be explained through two
20 possible mechanisms. First, the loss of protein expression of the polymerase subunits and
21 the nucleoprotein would make RNP formation impossible, which is the functional unit for
22 both transcription and vRNA replication. Secondly, the accumulation of the NP
23 monomeric pool has previously been shown to be a key molecular trigger in the switch
24 from transcription of mRNA to replication of vRNA in the viral life cycle.^{5,21,22} The loss
25 of this monomeric NP pool, evident in the size exclusion chromatography data (Figure
26
27
28
29
30
31
32
33
34
35
36
37
38
39
40
41
42
43
44
45
46
47
48
49
50
51
52
53
54
55
56
57
58
59
60

1
2
3 4b), could prevent this switch from occurring and thereby block vRNA synthesis from all
4
5 segments. These two mechanisms are not mutually exclusive, with each likely playing a
6
7 role in S119 inhibition of influenza virus replication. The observed differential inhibition
8
9 of mRNA expression by S119 from the three tested segments indicates a possible length-
10
11 dependent effect of the compound. An explanation for this phenomenon could again be
12
13 due to the loss of the monomeric NP pool. It has been well established that the viral
14
15 polymerase requires an NP-coated template for full processivity and that the lack of NP
16
17 will cause the polymerase to dissociate prematurely.²³ Absence of monomeric NP could
18
19 cause a reduction in NP-encapsidation of viral vRNAs resulting in reduced processivity
20
21 of the viral polymerase. It would be reasonable to infer that a loss of processivity would
22
23 disproportionately affect longer segments, as we observe in our experiments.
24
25
26
27
28
29

30
31 **Broad Spectrum Influenza A Virus Inhibition by S119 Analogs.** Our initial analysis
32
33 of the breadth of S119 anti-influenza virus activity indicated that it was only effective
34
35 against some H1N1 viruses with maximum potency observed against the A/WSN/33
36
37 laboratory strain and no effect on another H1N1 laboratory strain A/PR/8/34 (Table 1).
38
39 Due to this specificity, we performed a structure activity relationship study with a focus
40
41 on improving the antiviral breadth. Analogs of S119 were synthesized and screened for
42
43 activity against an influenza A/PuertoRico/8/34 virus expressing GFP²⁴, and to ensure we
44
45 were not selecting for H1N1 specific compounds, all analogs were counter screened
46
47 against an A/Vietnam/1203/2004 (H5N1) HALO GFP virus. Successive rounds of analog
48
49 production (66 in total), using an iterative process, resulted in increased potency against
50
51 the PR8 and H5N1 viruses. We found that activity against both the H1N1 and H5N1
52
53
54
55
56
57
58
59
60

1
2
3 viruses was also predictive of the ability to inhibit a representative H3N2 virus
4
5 (A/Panama/2007/1999). Therefore, we were confident that this screening process could
6
7 identify S119 analogs that had broad spectrum antiviral activity against influenza A
8
9 viruses, as listed in Table 1.

10
11 S119 is a symmetrical bis(4-*t*-butylphenyl)carboxamide of 1,4-diaminobenzene that
12
13 showed no detectable antiviral activity on the two influenza strains that were screened,
14
15 and a related symmetrical 1,3-benzenediamine analog S119-6 also showed narrow
16
17 spectrum activity. It is interesting to note that the unsymmetrical analogs, as in the
18
19 shortened mono-4-*tert*-butylphenyl carboxamide S119-2, the diphenyl ether bearing
20
21 carboxamide S119-3 or the diphenylamino analog S119-8, all possessed broader
22
23 spectrum anti-influenza activity as compared to S119. The analogs were designed to
24
25 explore the nature of the influenza activity pharmacophore as well as to improve
26
27 calculated physical chemical properties of the lipophilic (cLogP: 6.81), poorly soluble
28
29 S119 parent hit molecule. We plan to expand this SAR and will report on our progress in
30
31 future manuscripts.
32
33

34
35 Of these analogs, S119-8 demonstrated that it had acquired enhanced broad-spectrum
36
37 activity (Figure 7, Table 2) with improved calculated physical properties (i.e. lower clogP:
38
39 5.95), while maintaining significant potency ($IC_{50} = 1.43\mu M$) at non-toxic ($CC_{50} =$
40
41 $66.10\mu M$) concentrations, albeit somewhat higher (7-fold) than that of the parent S119
42
43 against WSN virus. Most interestingly, S119-8 also showed activity against multiple
44
45 influenza B viruses and an oseltamivir-resistant influenza A virus (Figure 7d, Table 2),
46
47 but did not inhibit a non-influenza virus, VSV (Figure S2). As evidence that S119-8 was
48
49
50
51
52
53
54
55
56
57
58
59
60

1
2
3 still targeting NP, we showed that the rWSN-Y40F virus maintained resistance to S119-8
4
5 (Figure S3).
6
7
8
9

10 **S119-8 Synergizes with oseltamivir.** Finally, future anti-influenza therapies are likely to
11 contain a cocktail of small molecules to deter the development of resistance²⁵. Therefore
12 it is important to understand how S119 interacts with currently licensed drugs and
13 potential influenza drugs in development. To this end, we tested the effect of the S119
14 analog S119-8 in combination with either nucleozin or oseltamivir. A549 cells were
15 infected with influenza PR8-GFP virus in the presence of the two compounds which were
16 titrated against each other in 3-fold serial dilutions starting with a concentration above the
17 IC₉₀ of each compound alone. Isobolograms of viral inhibition were generated (Figure 8)
18 and based on these data, the combination index for the S119-8-nucleozin interaction was
19 determined to be 0.79, suggesting an additive to slightly synergistic interaction. This was
20 somewhat surprising as we anticipated that the close proximity of the resistance
21 mutations of the two compounds could have potentially caused an antagonistic
22 interaction. When we examined the interaction between S119-8 and oseltamivir, we
23 found a combination index of 0.57 which indicates a synergistic relationship between the
24 two compounds. This implies that if the in vivo PK and safety profile of S119-8 is
25 acceptable, this compound would be a good candidate to include in a potential anti-
26 influenza drug cocktail by enhancing the potency of the current standard of care,
27 oseltamivir, and lowering the chances of developing resistance. Studies to improve the
28 antiviral and drug-like properties²⁶ of the S119 series are on-going.
29
30
31
32
33
34
35
36
37
38
39
40
41
42
43
44
45
46
47
48
49
50
51
52
53
54
55
56
57
58
59
60

Conclusion

The discovery of nucleozin has highlighted the viral nucleoprotein as a promising target for novel therapeutics against influenza virus. The highly conserved nature of the nucleoprotein^{27,28} and its critical importance in multiple stages of the viral life cycle make it an ideal target. Here we present S119 and its analog S119-8 as antiviral drug leads for the development of a pan-influenza NP inhibitor with a defined mechanism of action. Through a SAR study, S119-8 was shown to extend its breadth to multiple influenza A virus subtypes and even to influenza B viruses, therefore not suffering from the same specificity limitations as nucleozin. Furthermore, the rise in resistance to currently approved influenza antivirals has emphasized the potential benefits of antiviral cocktails for future therapeutics. The observed synergistic relationship between S119-8 and oseltamivir is encouraging for incorporation of such a compound (or improved derivatives) in future influenza antiviral drug cocktails.

Methods

Cell culture and reagents. Madin-Darby canine kidney (MDCK) epithelial cells, human alveolar epithelial (A549) cells, and human embryonic kidney 293T (293T) cells, were obtained from the American Type Culture Collection (ATCC, Manassas, VA). MDCK, A549, and 293T cells were cultured in Dulbecco's modified Eagle's medium (DMEM) (Gibco, Carlsbad, CA) supplemented with 10% fetal bovine serum (FBS) (HyClone, South Logan, UT), and 1% penicillin-streptomycin (P/S) (Gibco). All cells were grown at 37°C, 5% CO₂. Transfection of DNA was performed in Opti-MEM I-reduced serum medium (Opti-MEM) (Gibco) with Lipofectamine LTX (Invitrogen) in A549 cells

1
2
3 according to manufacturer's specifications.
4
5
6
7

8 **Expression plasmids and cloning.** The influenza virus plasmid pPolI-NP Y40F was
9
10 generated by exchanging one nucleotide in the parental plasmid pPolI-NP¹⁶ using the
11
12 QuickChange site-directed mutagenesis kit (Agilent Technologies, Wilmington, DE)
13
14 using specific primers (forward: 5'-
15
16 GATGGAATTGGACGATTCTTCATCCAAATGTGCACCGAAC -3'; reverse: 5'-
17
18 GTTCGGTGCACATTTGGATGAAGAATCGTCCAATTCCATC -3'). Presence of the
19
20 mutation was confirmed by sequencing (Macrogen, Rockville, MD). The mammalian
21
22 expression vector pCAGGS containing a chicken β -actin promoter has been previously
23
24 described.²⁹ Proper insertion and presence of the mutation was confirmed by sequencing
25
26
27
28
29 (Macrogen).
30
31
32

33 **Viruses.** The influenza A/WSN/1933 (H1N1) virus (WSN) was propagated in MDCK
34
35 cells for 2 days at 37°C. Influenza A/California/04/2009 (H1N1) virus was propagated in
36
37 MDCK cells for 3 days at 35°C. Influenza viruses A/Puerto Rico/8/1934 (H1N1) (PR8),
38
39 A/Brisbane/59/2007-S, A/Brisbane/59/2007-R, A/Wyoming/03/2003,
40
41 A/Panama/2007/1999 (H3N2) and A/Vietnam/1203/2004 (H5N1) bearing a mutated
42
43 polybasic cleavage site in the HA segment (HA₀) were propagated in 10-day old
44
45 embryonated chicken eggs for 2 days at 37°C. The A/Brisbane/59/2007-S and
46
47 A/Brisbane/59/2007-R viruses are oseltamivir sensitive (S) and resistant (R) versions of a
48
49 clinical isolate generated using a reverse genetics system as previously described³⁹ The
50
51 NS segment (A/Vietnam/1203/2004) carrying GFP was generated by overlapping fusion
52
53
54
55
56
57
58
59
60

1
2
3 PCR using standard molecular biology techniques. Briefly, the NS1 ORF without the stop
4 codon was fused to the N-terminal of a codon-optimized maxGFP (Amara) via a GSGG
5 linker region (NS1-GFP). The maxGFP was followed by a short GSG linker, a 19-aa 2A
6 autoproteolytic site (ATNFSLLKQAGDVEENPG↓P)³⁴—derived from porcine
7 teschovirus-1 and by the NEP ORF. Also, silent mutations in the endogenous splice
8 acceptor site in the NS1 ORF were introduced to prevent splicing.³⁵ The engineered NS-
9 GFP segment was cloned in the pDZ IAV rescue plasmid.³⁶ Influenza
10 B/Yamagata/16/1988 and B/Brisbane/60/2008 viruses was propagated in 8-day old
11 embryonated chicken eggs for 3 days at 33°C. All influenza viruses were titered by
12 standard plaque assay in MDCK cells. Vesicular stomatitis virus was grown and titered
13 by plaque assay in VERO cells. Recombinant influenza viruses were generated using the
14 influenza virus rescue protocol as previously described.¹⁶ Briefly, 293T cells were
15 transfected with eight pPolI constructs expressing the PB1, PB2, PA, NP (or NP Y40F),
16 HA, NA, M, and NS genomic segments as well as pCAGGS expression plasmids
17 encoding the PB1, PB2, PA, and NP proteins. Twenty four hours post transfection,
18 MDCK cells were co-cultured with the transfected 293Ts for an additional 24–48 hours,
19 until cytopathic effects were observed. Newly generated viruses were collected and
20 plaque-purified, and the presence of the mutation was confirmed by sequencing.
21
22
23
24
25
26
27
28
29
30
31
32
33
34
35
36
37
38
39
40
41
42
43
44
45
46

47 **Small molecular weight compounds.** Nucleozin was purchased from Sigma Aldrich (St.
48 Louis, MO). The active VX-787 analog and oseltamivir carboxylate were kindly
49 provided as gifts by Roche (Basel, Switzerland). Compounds were purchased through
50 eMolecules (La Jolla, CA) and dissolved in 100% DMSO. The final concentration of
51
52
53
54
55
56
57
58
59
60

1
2
3 DMSO in the culture medium did not exceed 0.5%.
4
5
6
7

8 **Cell viability assay.** The CellTiterGlo Cell Viability Assay (Promega) was used to detect
9
10 ATP levels as a function of cell viability, according to manufacturer's specifications.
11
12 A549 cells were seeded into 96-well plates (1250 cells/well) and incubated at 37°C, 5%
13
14 CO₂ for 24 hours. Culture medium was then replaced with 100 uL of fresh medium
15
16 containing compound (serially diluted), and this was further incubated for 24 hours. Cell
17
18 viability was measured by adding 50 uL of CellTiterGlo reagent to each well, and the
19
20 luminescence signal was read using a plate reader (Beckman Coulter, Brea, CA). The
21
22 CC₁₀ and CC₅₀ for each experiment were determined using the Prism (GraphPad
23
24 Software) software.
25
26
27
28
29

30
31 **Viral growth assays in the presence of inhibitors.** 100,000 A549 cells were seeded into
32
33 24-well plates and incubated for 24 h at 37 °C, 5% CO₂. Two hours before infection, the
34
35 medium was replaced with DMEM containing the compound of interest at the indicated
36
37 concentrations. Compounds were absent during the 1-h virus incubation but were present
38
39 in the DMEM post-infection medium. Infections were performed at a low MOI (0.01-0.1)
40
41 for 24 or 48 hours, depending on virus used. For infections with influenza viruses, post-
42
43 infection medium also contained 1 ug/mL TPCK-treated trypsin (Sigma-Aldrich, St.
44
45 Louis, MO). The infected cells were incubated at 37 °C with the exception of influenza B
46
47 virus-infected cells, which were incubated at 33 °C. Viral titers were determined by
48
49 standard plaque assay in MDCK cells. The IC₅₀ and IC₉₀ for each experiment were
50
51 determined using the Prism (GraphPad Software) software.
52
53
54
55
56
57

Selection of S119-resistant influenza viruses.

The concentration of S119 required for maximum virus inhibition (3 logs), while maintaining enough virus production for subsequent passages was determined (2 μ M S119). A549 cells were infected with WSN at an MOI of 0.01 for 24 hours at 37°C under S119 treatment. The supernatant was then collected and titered by plaque assay. If the recovered S119 treated virus did not show increased viral titer similar to that of the DMSO treated control, the virus was passaged again by same method. Once increased titers in the presence of S119 were detected for two consecutive passages, the viruses were plaque purified. Following plaque purification, all 8 genome segments were sequenced and compared to DMSO treated control virus to detect escape mutations.

Blue native PAGE

Blue Native PAGE was used to examine the effect of S119 on the multimeric state of the NP proteins. Purified recombinant wild-type WSN NP protein was kindly produced by Florian Krammer as previously described^{37,38} and 5 μ g of purified protein was incubated with 10 μ M S119 at 25° C for 30 min. 1 μ g of purified influenza virus RNA or Nuclease-free water was added, up to 10 μ l. After an additional incubation of 15 minutes at 25° C, the samples were mixed with 2.5 μ l of 5% Coomassie brilliant blue G-250 and loaded into sample wells of nondenaturing 4–20% gradient Mini-Protean TGX gel (Bio-Rad). Samples were separated by electrophoresis at a constant voltage of 150 V for 60 min at 25° C in a blue native Tris/Glycine buffer system (Coomassie brilliant blue G-250 0.02% Cathode Buffer). Gels were destained with 25% methanol/10% acetic acid solution and visualized using the Bio-Rad (Hercules, CA) ChemiDoc MP Imaging System.

Size exclusion chromatography

To determine the oligomerization state of NP, A549 cells were infected with WSN virus (MOI = 1) in the presence or absence of 10 μ M S119 or 1 μ M Nucleozin for 24 hours. Cells were then lysed in 50 mM Tris-HCl, 100 mM KCl, 5 mM MgCl₂ and 0.5% NP40 containing protease and phosphatase inhibitor cocktails. Total cell extract was clarified by centrifugation, treated with 50 μ g/ml of RNase A for 2 hours at room temperature, and fractionated through a Superose-6 column pre-equilibrated in lysis buffer. Fractions were probed by western blotting with an anti-NP (HT103) antibody.

Immunofluorescence microscopy

A549 cells were grown to 70–80% confluency on coverslips. Cells were infected for 2 h at MOI = 5 in the presence or absence of 10 μ M S119 or 1 μ M Nucleozin and washed. S119 was maintained in culture throughout the experiment. Infections were stopped at indicated time points by fixation in methanol for 30 min at 4C. Cells were blocked with 1% BSA for 30 minutes and then were incubated for 1h with primary antibodies against NP (HT103) in PBS (dilution 1:2000), washed and stained with Alexa Fluor 488-conjugated secondary antibodies (Invitrogen) (dilution 1:1000) for 1h. Coverslips were then washed and counterstained with 4',6-diamidino-2-phenylindole, dihydrochloride (DAPI) (Invitrogen) for nucleus localization and mounted on slides using Prolong Gold antifade mounting medium (Invitrogen) before image analysis by fluorescence microscopy.

Fluorescent primer extension assay

Primer extension of influenza RNA was performed using 5'-end labeled fluorescent primers with either Alexa Fluor 488 for vRNA detection or Alexa Fluor 546 for m/cRNA detection of the PB2 (vRNA: 5'- TGCTAATTGGGCAAGGAGAC -3' or m/cRNA: 5'- GCCATCATCCATTTCATCCT -3'), NP (vRNA: 5'- TGATGGAAAGTGCAAGACCA -3' or m/cRNA: 5'- TGATTTTCAGTGGCATTCTGG -3'), and NS (vRNA: 5'- TGATTGAAGAAGTGAGACACAG -3' or m/cRNA: 5'- CGCTCCACTATTTGCTTTCC -3'), segments. An Alexa Fluor 488 5'-labeled primer targeting the human 5S rRNA (5'- TCCCAGGCGGTCTCCCATCC -3') was used as a loading control. A549 cells were pretreated for 2 hours with S119, VX-787, or DMSO and infected with the WSN virus for 6 hours (MOI 5) under continued compound treatment. Infected A549 total RNA (100 ug) was added to the fluorescent primer (10 pmol), heated to 90°C (3 min), and cooled on ice. Reverse transcription (RT) reactions were performed in 50 mM Tris-HCl (pH 8.3), 75 mM KCl, 5 mM MgCl₂, and 10 mM DTT with 0.5 mM each dNTP. 50U SuperScript III (Invitrogen) was added and reactions were incubated at 45°C for 60 min. cDNA samples were mixed with an equal volume of loading dye solution (Formamide, 5mM EDTA pH 8, 1% bromophenol blue) and heated to 95°C for 3 minutes to stop the reaction. Samples were loaded on a 6% polyacrylamide gel containing 7M Urea in TBE buffer. Gel Fluorescence was detected using the Bio-Rad (Hercules, CA) ChemiDoc MP Imaging System.

Antiviral combination assay

The combined antiviral effect of S119-8 (S119 Analog) and nucleozin or oseltamivir

1
2
3 carboxylate was tested against the A/Puerto Rico/8/34 strain expressing GFP from
4 segment 8 (PR8-GFP), which has been previously described.²⁴ A549 cells were infected
5 with PR8-GFP (MOI = 0.01) in the presence or absence of multiple drug combinations
6 for 24 hours. The concentration of the drugs used was based on their respective 50%
7 inhibitory concentrations (IC₅₀) against PR8-GFP in A549 cells. The assays were
8 performed in 96-well format using a liquid handling robot (Biomex NXP, Beckman) to
9 ensure accuracy. Infected cells were detected through GFP fluorescence, quantified by
10 laser scanning cytometry (Acumen, TTP Labtech). Isobolograms and combination
11 indices were calculated as previous described.³⁰
12
13
14
15
16
17
18
19
20
21
22
23
24
25

26 **Synthesis of S119 and related analogs**

27
28 **N,N'-(1,4-phenylene)bis(4-(tert-butyl)benzamide) (S119):** To a solution of 1,4-
29 diamino-benzene **2c** (0.07g, 1 equiv.), triethylamine (3.0 equiv.) in CH₂Cl₂ was added 4-
30 (1,1-dimethylethyl)benzoyl chloride **1** (2.2 equiv.) at 0°C. The resulted white suspension
31 was stirred at room temperature for 12 h and then filtered. The white cake was washed
32 with CH₂Cl₂ (10 mL), EtOH (10 mL) and dried under vacuum to give the desired product
33 **8** as white powder 0.2g (72% yield). ¹H-NMR (600 MHz, d₆-DMSO): δ 10.17 (s,2H),
34 7.90-7.89 (d, 4H), 7.74 (m, 4H), 7.56-7.54 (d, 4H), 1.33 (s, 18H); ¹³C NMR (125 MHz,
35 d₆-DMSO): δ 165.2, 154.3, 134.9, 132.3, 127.4, 125.1, 120.5, 34.7, 30.9; LCMS (tof+)
36 for C₂₈H₃₂N₂O₂ [M] 428.2464; Found [M+ H]⁺ for 429.2538
37
38
39
40
41
42
43
44
45
46
47
48
49
50

51 **Synthesis of S119-8: 4-(tert-butyl)-N-(4-(phenylamino)phenyl)benzamide (S119-8):**
52
53
54
55
56
57
58
59
60

1
2
3 **Step 1: N-(4-aminophenyl)-4-(tert-butyl)benzamide:** To a solution of 1,4-diamino-
4 benzene (0.42g, 1.2 equiv.), triethylamine (1.5 equiv.) in CH₂Cl₂ was added 4-(1,1-
5 dimethylethyl)benzoyl chloride **1** (1.0 equiv.) at 0°C. The resulted white suspension was
6 stirred at room temperature for 12 h and then filtered. Product was purified via flash
7 chromatography (gradient elution from 40% EtOAc in Hexanes to 60% EtOAc in
8 Hexanes) to give product as light yellow powder 0.6g (70% yield). ¹H-NMR (600 MHz,
9 CDCl₃): δ 7.97 (s, 1H), 7.80-7.79 (d, 2H), 7.46-7.45 (d, 2H), 7.40-7.39 (d, 2H), 6.67-6.66
10 (d, 2H), 3.58 (s, 2H), 1.35 (s, 9H); ¹³C NMR (125 MHz, CDCl₃): δ 165.2, 154.5, 142.8,
11 131.8, 129.0, 126.4, 125.1, 121.9, 115.1, 34.5, 30.7; LCMS (tof+) for C₁₇H₂₀N₂O [M]
12 268.1576; Found [M+ H]⁺ for 269.1654.

13
14
15
16
17
18
19
20
21
22
23
24
25
26 **Step 2:** To a solution of N-(4-aminophenyl)-4-(tert-butyl)benzamide (0.115g, 1.0
27 equiv.), BiPh₃ (0.19 g, 1.01 equiv.) and Cu(OAc)₂ (0.08g, 1.0 equiv.) in CH₂Cl₂ (20 mL)
28 was added with triethylamine (0.07mL, 0.48 mmol, 1.1 equiv.) at room temperature.³¹
29 The resulted suspension was stirred at room temperature for 16 h before diluted with
30 CH₂Cl₂ (20 mL), followed by addition of 1N HCl (12 mL) and kept stirring for 1 h. The
31 organic layer was separated, washed with 1N HCl (20 mL) and dried over K₂CO₃. After
32 filtration, the filtrate was concentrated and purified via flash chromatography (gradient
33 elution from 10% EtOAc in Hexanes to 25% EtOAc in Hexanes) to give product as
34 brown solid 0.1g (71 % yield). ¹H-NMR (600 MHz, CDCl₃): δ 8.00 (s, 1H), 7.84-7.83 (d,
35 2H), 7.55-7.54 (d, 2H), 7.23 (t, 2H), 7.08-7.04 (dd, 4H), 6.94 (t, 1H), 1.37 (s, 9H); ¹³C
36 NMR (125 MHz, CDCl₃): δ 165.3, 154.8, 143.0, 139.2, 131.6, 131.2, 128.9, 126.4, 125.2,
37 121.5, 120.2, 118.4, 116.7, 34.5, 30.7 ; LCMS (tof+) for C₂₃H₂₄N₂O [M] 344.1889;
38 Found [M+ H]⁺ for 345.1956.

1
2
3
4
5 Similar procedures as for S119 were used to prepared related analogs.
6

7
8 **S119-2: 4-(tert-butyl)-N-(4-(tert-butyl)phenyl)benzamide (S119-2)** To a solution of 4-
9
10 tert-butylaniline (0.23g, 1.54 mmol, 1.0 equiv.) and triethylamine (0.16 g, 1.54 mmol, 1.0
11
12 equiv.) in CH₂Cl₂ (20 mL) was added with 4-(1,1-dimethylethyl)benzoyl chloride (0.28g,
13
14 1.54 mmol, 1.0 equiv.) at 0°C. The resulted white suspension was stirred at room
15
16 temperature for 12 h and then filtered. The filtrate was concentrated and purified via flash
17
18 chromatography (gradient elution from 0% EtOAc in Hexanes to 4% EtOAc in Hexanes)
19
20 to give product as white powder 0.46g (95% yield). ¹H-NMR (600 MHz, CDCl₃): δ 7.98
21
22 (s,1H), 7.83-7.82 (d, 2H), 7.60-59 (d, 2H), 7.49-7.48 (d, 2H), 7.40-7.39 (d, 2H), 1.36 (s,
23
24 9H), 1.35 (s, 9H); ¹³C NMR (125 MHz, CDCl₃): δ 165.2, 154.8, 146.9, 135.0, 131.7,
25
26 126.4, 125.4, 125.2, 119.5, 34.5, 33.9, 30.9, 30.7; LCMS (tof+) for C₂₁H₂₇NO;^[M]
27
28 309.2093; Found <sup>[M+ H]⁺ for 310.2158
29
30
31
32
33
34</sup>

35
36 **S119-3: 4-(tert-butyl)-N-(4-phenoxyphenyl)benzamide (3b):** Prepared as above from
37
38 4-phenoxy-phenylamine **2b** (0.10g, 1.0 equiv.), triethylamine (1.0 equiv.) and 4-(1,1-
39
40 dimethylethyl)benzoyl chloride **1** (1.0 equiv.) Product was purified via flash
41
42 chromatography (gradient elution from 0% EtOAc in Hexanes to 8% EtOAc in Hexanes)
43
44 to give product as white powder 0.18g (96% yield). ¹H-NMR (600 MHz, CDCl₃): δ 8.05
45
46 (s, 1H), 7.84-7.82 (d,2H), 7.63-7.62 (d, 2H), 7.50-7.48 (d, 2H), 7.35 (t, 1H), 7.11 (t, 1H),
47
48 7.03-7.01 (m, 3H), 1.37 (s, 9H); ¹³C NMR (125 MHz, CDCl₃): δ 165.3, 157.1, 154.9,
49
50 153.1, 133.1, 131.5, 129.3, 126.5, 125.2, 122.6, 121.6, 119.2, 117.9, 34.5, 30.7; LCMS
51
52 (tof+) for C₂₃H₂₃NO₂ ^[M] 345.1729; Found <sup>[M+ H]⁺ for 346.1787.
53
54
55
56
57</sup>

1
2
3
4
5
6 S119-6: **N,N'-(1,3-phenylene)bis(4-(tert-butyl)benzamide) (S119-6)**: Prepared as
7
8 above from 1,3-diamino-benzene (0.10g, 1.0 equiv.), triethylamine (3.0 equiv.) and 4-
9
10 (1,1-dimethylethyl)benzoyl chloride **1** (2.2 equiv.). Product was purified via flash
11
12 chromatography (gradient elution from 0% EtOAc in Hexanes to 25% EtOAc in
13
14 Hexanes) to give product as white powder 0.3g (77% yield). ¹H-NMR (600 MHz,
15
16 CDCl₃): δ 8.13 (s, 1H), 8.02-7.94 (m, 2H), 7.82-7.81 (m, 4H), 7.51-7.48 (m, 6H), 7.38-
17
18 7.34 (m, 1H), 1.38-1.38 (d, 18H); ¹³C NMR (125 MHz, CDCl₃): δ 165.3, 155.1, 138.3,
19
20 131.4, 129.2, 126.4, 125.3, 115.3, 110.9, 34.5, 30.7; LCMS (tof+) for C₂₈H₃₂N₂O₂ [M]
21
22 428.2464; Found [M+ H]⁺ for 429.2523.
23
24
25
26
27
28

29 **Supporting Information**

- 30
31 - Figure S1 presents size exclusion chromatography data from infected cell extracts
32
33 treated with S119 or nucleozin in the absence of RNase treatment.
34
- 35 - Figure S2 shows that S119-8 does not inhibit VSV and is a specific inhibitor of
36
37 influenza viruses.
38
- 39 - Figure S3 shows that S119-8 retains the same Y40F resistant phenotype as the
40
41 parental S119.
42
43
44
45
46

47 **Abbreviations**

48
49 VSV - Vesicular Stomatitis Virus, SAR - Structure Activity Relationship, IC₅₀ - 50%
50
51 Inhibitory Concentration, IC₉₀ - 90% Inhibitory Concentration, CC₅₀ - 50% Cytotoxic
52
53 Concentration, CC₁₀ - 10% Cytotoxic Concentration
54
55
56
57

Author Information

¹Department of Microbiology, ²Department of Pharmacological Sciences, ³Immunity and Pathogenesis Program, Infectious and Inflammatory Disease Center, Sanford Burnham Prebys Medical Discovery Institute, 10901 North Torrey Pines Road, La Jolla, California 92037, USA, ⁴Department of Medicine, Division of Infectious Diseases, ⁵Global Health and Emerging Pathogens Institute, ⁶Drug Discovery Institute, Icahn School of Medicine at Mount Sinai, New York, NY 10029, USA,

[^]Present Address: Suzhou Novartis Pharma Technology Co., Ltd. 18 Tonglian Road, Riverside Industrial Park, Changshu Economic Development Zone, Changshu / Jiangsu Province 215537, China.

[#]Present Address: Department of Microbiology, University of Chicago, Chicago, Illinois, USA.

*Corresponding author

Department of Microbiology
Icahn School of Medicine at Mount Sinai
One Gustave L. Levy Place
New York, NY 10029, USA.

Tel.: +1-212-241-8931

megan.shaw@mssm.edu

Conflict of Interest

None to Report

Acknowledgements

We thank Dr. Florian Krammer for producing the purified NP proteins. JChem for Excel was used for structure database management, search, and prediction, JChem for Excel 6.1.1, 2013, ChemAxon (<http://www.chemaxon.com>). This work was supported in part by National Institutes of Health (NIH) Grants U01AI1074539, R21AI102169 and U19AI106754 and a Mount Sinai seed fund to the Devita laboratory. This work was also partially supported by CRIP (Center for Research on Influenza Pathogenesis), an NIAID-funded Center of Excellence for Influenza Research and Surveillance (CEIRS, HHSN272201400008C).

References

1. Dong G, Peng C, Luo J, Wang C, Han L, Wu B, Ji G, He H. Adamantane-resistant influenza A viruses in the world (1902-2013): frequency and distribution of M2 gene mutations. *PLoS One* 2015, 10:e0119115, doi:10.1371/journal.pone.0119115.
2. Whitley RJ, Boucher CA, Lina B, Nguyen-Van-Tam JS, Osterhaus A, Schutten M, Monto AS. Global assessment of resistance to neuraminidase inhibitors, 2008-2011: the Influenza Resistance Information Study (IRIS). *Clin Infect Dis* 2013, 56:1197-1205, doi:10.1093/cid/cis1220.
3. Arranz R, Coloma R, Chichon FJ, Conesa JJ, Carrascosa JL, Valpuesta JM, Ortin J, Martin-Benito J. The structure of native influenza virion ribonucleoproteins. *Science* 2012, 338:1634-1637, doi:10.1126/science.1228172.
4. Amorim MJ, Bruce EA, Read EK, Foeglein A, Mahen R, Stuart AD, Digard P. A Rab11- and microtubule-dependent mechanism for cytoplasmic transport of influenza A virus viral RNA. *J Virol* 2011, 85:4143-4156, doi:10.1128/JVI.02606-10.
5. Newcomb LL, Kuo RL, Ye Q, Jiang Y, Tao YJ, Krug RM. Interaction of the influenza A virus nucleocapsid protein with the viral RNA polymerase potentiates unprimed viral RNA replication. *J Virol* 2009, 83:29-36, doi:10.1128/JVI.02293-07.

- 1
 - 2
 - 3
 - 4
 - 5
 - 6
 - 7
 - 8
 - 9
 - 10
 - 11
 - 12
 - 13
 - 14
 - 15
 - 16
 - 17
 - 18
 - 19
 - 20
 - 21
 - 22
 - 23
 - 24
 - 25
 - 26
 - 27
 - 28
 - 29
 - 30
 - 31
 - 32
 - 33
 - 34
 - 35
 - 36
 - 37
 - 38
 - 39
 - 40
 - 41
 - 42
 - 43
 - 44
 - 45
 - 46
 - 47
 - 48
 - 49
 - 50
 - 51
 - 52
 - 53
 - 54
 - 55
 - 56
 - 57
 - 58
 - 59
 - 60
6. Turrell L, Lyall JW, Tiley LS, Fodor E, Vreede FT. The role and assembly mechanism of nucleoprotein in influenza A virus ribonucleoprotein complexes. *Nat Commun* 2013, 4:1591, doi:10.1038/ncomms2589.
7. Noton SL, Medcalf E, Fisher D, Mullin AE, Elton D, Digard P. Identification of the domains of the influenza A virus M1 matrix protein required for NP binding, oligomerization and incorporation into virions. *J Gen Virol* 2007, 88:2280-2290, doi:10.1099/vir.0.82809-0.
8. Ashour J, Schmidt FI, Hanke L, Cragolini J, Cavallari M, Altenburg A, Brewer R, Ingram J, Shoemaker C, Ploegh HL. Intracellular expression of camelid single-domain antibodies specific for influenza virus nucleoprotein uncovers distinct features of its nuclear localization. *J Virol* 2015, 89:2792-2800, doi:10.1128/JVI.02693-14.
9. Moeller A, Kirchdoerfer RN, Potter CS, Carragher B, Wilson IA. Organization of the influenza virus replication machinery. *Science* 2012, 338:1631-1634, doi:10.1126/science.1227270.
10. Kakisaka M, Sasaki Y, Yamada K, Kondoh Y, Hikono H, Osada H, Tomii K, Saito T, Aida Y. A Novel Antiviral Target Structure Involved in the RNA Binding, Dimerization, and Nuclear Export Functions of the Influenza A Virus Nucleoprotein. *PLoS Pathog* 2015, 11:e1005062, doi:10.1371/journal.ppat.1005062.
11. Kao RY, Yang D, Lau LS, Tsui WH, Hu L, Dai J, Chan MP, Chan CM, Wang P, Zheng BJ, et al. Identification of influenza A nucleoprotein as an antiviral target. *Nat Biotechnol* 2010, 28:600-605, doi:10.1038/nbt.1638.
12. Gerritz SW, Cianci C, Kim S, Pearce BC, Deminie C, Discotto L, McAuliffe B, Minassian BF, Shi S, Zhu S, et al. Inhibition of influenza virus replication via small molecules that induce the formation of higher-order nucleoprotein oligomers. *Proc Natl Acad Sci U S A* 2011, 108:15366-15371, doi:10.1073/pnas.1107906108.
13. White KM, De Jesus P, Chen Z, Abreu P, Jr., Barile E, Mak PA, Anderson P, Nguyen QT, Inoue A, Stertz S, et al. A Potent Anti-influenza Compound Blocks Fusion through Stabilization of the Prefusion Conformation of the Hemagglutinin Protein. *ACS Infect Dis* 2015, 1:98-109, doi:10.1021/id500022h.
14. Konig R, Stertz S, Zhou Y, Inoue A, Hoffmann HH, Bhattacharyya S, Alamares JG, Tscherne DM, Ortigoza MB, Liang Y, et al. Human host factors required for influenza virus replication. *Nature* 2010, 463:813-817, doi:10.1038/nature08699.
15. Pang B, Cheung NN, Zhang W, Dai J, Kao RY, Zhang H, Hao Q. Structural Characterization of H1N1 Nucleoprotein-Nucleozin Binding Sites. *Sci Rep* 2016, 6:29684, doi:10.1038/srep29684.
16. Martinez-Sobrido L, Garcia-Sastre A. Generation of recombinant influenza virus from plasmid DNA. *J Vis Exp* 2010, doi:10.3791/2057.
17. Ng AK, Zhang H, Tan K, Li Z, Liu JH, Chan PK, Li SM, Chan WY, Au SW, Joachimiak A, et al. Structure of the influenza virus A H5N1 nucleoprotein: implications for RNA binding, oligomerization, and vaccine design. *FASEB J* 2008, 22:3638-3647, doi:10.1096/fj.08-112110.
18. Tarus B, Bakowicz O, Chenavas S, Duchemin L, Estrozi LF, Bourdieu C, Lejal N, Bernard J, Moudjou M, Chevalier C, et al. Oligomerization paths of the

- nucleoprotein of influenza A virus. *Biochimie* 2012, 94:776-785, doi:10.1016/j.biochi.2011.11.009.
19. Ye Q, Krug RM, Tao YJ. The mechanism by which influenza A virus nucleoprotein forms oligomers and binds RNA. *Nature* 2006, 444:1078-1082, doi:10.1038/nature05379.
20. Byrn RA, Jones SM, Bennett HB, Bral C, Clark MP, Jacobs MD, Kwong AD, Ledebor MW, Leeman JR, McNeil CF, et al. Preclinical activity of VX-787, a first-in-class, orally bioavailable inhibitor of the influenza virus polymerase PB2 subunit. *Antimicrob Agents Chemother* 2015, 59:1569-1582, doi:10.1128/AAC.04623-14.
21. Portela A, Digard P. The influenza virus nucleoprotein: a multifunctional RNA-binding protein pivotal to virus replication. *J Gen Virol* 2002, 83:723-734, doi:10.1099/0022-1317-83-4-723.
22. Vreede FT, Jung TE, Brownlee GG. Model suggesting that replication of influenza virus is regulated by stabilization of replicative intermediates. *J Virol* 2004, 78:9568-9572, doi:10.1128/JVI.78.17.9568-9572.2004.
23. Honda A, Ueda K, Nagata K, Ishihama A. RNA polymerase of influenza virus: role of NP in RNA chain elongation. *J Biochem* 1988, 104:1021-1026.
24. Manicassamy B, Manicassamy S, Belicha-Villanueva A, Pisanelli G, Pulendran B, Garcia-Sastre A. Analysis of in vivo dynamics of influenza virus infection in mice using a GFP reporter virus. *Proc Natl Acad Sci U S A* 2010, 107:11531-11536, doi:10.1073/pnas.0914994107.
25. van der Vries E, Schutten M, Fraaij P, Boucher C, Osterhaus A. Influenza virus resistance to antiviral therapy. *Adv Pharmacol* 2013, 67:217-246, doi:10.1016/B978-0-12-405880-4.00006-8.
26. Meanwell NA. Improving drug candidates by design: a focus on physicochemical properties as a means of improving compound disposition and safety. *Chem Res Toxicol* 2011, 24:1420-1456, doi:10.1021/tx200211v.
27. Kukol A, Hughes DJ. Large-scale analysis of influenza A virus nucleoprotein sequence conservation reveals potential drug-target sites. *Virology* 2014, 454-455:40-47, doi:10.1016/j.virol.2014.01.023.
28. Babar MM, Zaidi NU. Protein sequence conservation and stable molecular evolution reveals influenza virus nucleoprotein as a universal druggable target. *Infect Genet Evol* 2015, 34:200-210, doi:10.1016/j.meegid.2015.06.030.
29. Niwa H, Yamamura K, Miyazaki J. Efficient selection for high-expression transfectants with a novel eukaryotic vector. *Gene* 1991, 108:193-199.
30. Chou TC. Theoretical basis, experimental design, and computerized simulation of synergism and antagonism in drug combination studies. *Pharmacol Rev* 2006, 58:621-681, doi:10.1124/pr.58.3.10.
31. Sorenson RJ. Selective N-arylation of aminobenzanilides under mild conditions using triaryl bismuthanes. *J Org Chem* 2000, 65:7747-7749.
32. Morens DM, Taubenberger JK, Harvey HA, Memoli MJ. The 1918 influenza pandemic: lessons for 2009 and the future. *Crit Care Med* 2010, 38:e10-20, doi:10.1097/CCM.0b013e3181ceb25b.
33. Belongia EA, Simpson MD, King JP, Sundaram ME, Kelley NS, Osterholm MT, McLean HQ. Variable influenza vaccine effectiveness by subtype: a systematic

- 1
2
3 review and meta-analysis of test-negative design studies. *Lancet Infect Dis* 2016,
4 16:942-951, doi:10.1016/S1473-3099(16)00129-8.
- 5 34. Basler CF, Reid AH, Dybing JK, Janczewski TA, Fanning TG, Zheng H,
6 Salvatore M, Perdue ML, Swayne DE, Garcia-Sastre A, et al. Sequence of the
7 1918 pandemic influenza virus nonstructural gene (NS) segment and
8 characterization of recombinant viruses bearing the 1918 NS genes. *Proc Natl*
9 *Acad Sci U S A* 2001, 98:2746-2751, doi:10.1073/pnas.031575198.
- 10 35. Donnelly ML, Hughes LE, Luke G, Mendoza H, ten Dam E, Gani D, Ryan MD.
11 The 'cleavage' activities of foot-and-mouth disease virus 2A site-directed mutants
12 and naturally occurring '2A-like' sequences. *J Gen Virol* 2001, 82:1027-1041,
13 doi:10.1099/0022-1317-82-5-1027.
- 14 36. Quinlivan M, Zamarin D, Garcia-Sastre A, Cullinane A, Chambers T, Palese P.
15 Attenuation of equine influenza viruses through truncations of the NS1 protein. *J*
16 *Virology* 2005, 79:8431-8439, doi:10.1128/JVI.79.13.8431-8439.2005.
- 17 37. Krammer F, Schinko T, Palmberger D, Tauer C, Messner P, Grabherr R.
18 *Trichoplusia ni* cells (High Five) are highly efficient for the production of influenza
19 A virus-like particles: a comparison of two insect cell lines as production
20 platforms for influenza vaccines. *Mol Biotechnol* 2010, 45:226-234,
21 doi:10.1007/s12033-010-9268-3.
- 22 38. Pica N, Hai R, Krammer F, Wang TT, Maamary J, Eggink D, Tan GS, Krause JC,
23 Moran T, Stein CR, et al. Hemagglutinin stalk antibodies elicited by the 2009
24 pandemic influenza virus as a mechanism for the extinction of seasonal H1N1
25 viruses. *Proc Natl Acad Sci U S A* 2012, 109:2573-2578,
26 doi:10.1073/pnas.1200039109.
- 27 39. Bouvier NM, Rahmat S, Pica N. Enhanced mammalian transmissibility of
28 seasonal influenza A/H1N1 viruses encoding an oseltamivir-resistant
29 neuraminidase. *J Virol* 2012, 86:7268-7279, doi:10.1128/JVI.07242-12.
30
31
32
33
34
35
36
37
38

39 **Figure 1. S119 potently inhibits influenza A virus.** (a) Chemical structure of compound
40 S119 and its molecular weight (MW). (b) MDCK or (c) A549 cells were infected with
41 influenza A/WSN/33 virus (MOI = 0.01) in the presence of serially diluted S119. Viral
42 titers were determined 24 hours post infection (solid line) and the IC₅₀ and IC₉₀ were
43 calculated. Cell viability was determined in an independent experiment in A549 cells
44 over a 24 hour period (dashed-line) and the CC₅₀ and CC₁₀ were calculated. Mean of
45 three replicates ± SD are shown.
46
47
48
49
50
51
52
53
54
55
56
57
58
59
60

1
2
3 **Figure 2. S119 inhibits a post-entry stage of the viral life cycle.** Time-of-addition assay
4 for inhibition of influenza A/WSN/33 virus by S119. A549 cells were infected with
5 influenza virus A/WSN/33 (MOI = 1). Compound S119 (10 μ M) was present in the
6 culture medium 2 h before infection or added to the medium at the indicated time points
7 post-infection. Viral titers were determined 24 h post-infection by plaque assay. The
8 assay was performed in triplicate; results are presented as the mean \pm SD.
9
10
11
12
13
14
15
16
17
18

19 **Figure 3. Resistance mutations to S119 occur within the nucleoprotein.** (a) Crystal
20 structure of A/WSN/33 NP (PDB 2IQH) monomer. Residue positions where S119 escape
21 mutations occurred are indicated in green. Virus titers from A549 cells infected with
22 either rWSN-WT or rWSN-NP/Y40F viruses (MOI = 0.01) in the presence of increasing
23 concentrations of (b) S119 or (c) nucleozin for 24 h. Curves represent means of triplicate
24 values \pm SD. IC₅₀ and IC₉₀ values are indicated.
25
26
27
28
29
30
31
32
33
34

35 **Figure 4. S119 alters the oligomerization state of NP.** (a) Visualization and
36 comparison of the effects of S119 and nucleozin on purified recombinant wild-type NP in
37 the absence and presence of RNA; native gradient gel conditions, stained with Coomassie
38 brilliant blue G-250. All samples were loaded on the same gel and an irrelevant
39 experimental compound originally in the 4th lane was removed resulting in the split
40 figure. Size exclusion chromatography was performed on cell extract from A549 cells
41 infected with (b) A/WSN/33 virus or (c) rY40F WSN virus and treated with either S119
42 or nucleozin. Extracts were RNase treated, applied to a Superose6 column, and 1ml
43 fractions were collected and analyzed by western blot for NP content.
44
45
46
47
48
49
50
51
52
53
54
55
56
57
58
59
60

1
2
3
4
5
6 **Figure 5. Large aggregates of NP accumulate in the cytoplasm upon S119 treatment.**

7
8 A549 cells infected with A/WSN/33 virus were treated with S119 or nucleozin and NP
9
10 localization was tracked at 2, 4, 6 and 24hrs. DAPI staining and mouse anti-influenza A
11
12 NP antibodies were used to define the locations of the nucleus and NP respectively.
13
14
15
16

17 **Figure 6. NP aggregation leads to alterations in viral RNA expression.** A549 cells

18
19 infected with either A/WSN/33 (a-c) virus or the mutant rWSN-Y40F (d-f) virus were
20
21 treated with S119, nucleozin or VX-787 control for 24 hours. Viral mRNA and vRNA
22
23 were detected using a primer extension assay with 5S ribosomal RNA serving as a
24
25 loading control. Protein expression was monitored through western blot for the
26
27 expression of (a + d) PB2, (b + e) NP, and (c + f) NS1, with GAPDH as a loading
28
29 control.
30
31
32
33
34

35 **Figure 7. S119-8 has increased antiviral breadth.** A549 cells were infected with

36
37 influenza (a) A/Panama/2007/1999 (H3N2, MOI = 0.01, 24 hours), (b)
38
39 A/California/04/2009 (H1N1, MOI = 0.1, 48 hours) or (c) A/Vietnam/1203/2004 (H5N1-
40
41 HaLo, MOI = 0.01, 24 hours) or (d) MDCK cells were infected B/Yamagata/16/1988
42
43 (MOI = 0.1, 48 hours) in the presence of serially diluted S119-8. Viral titers were
44
45 determined and represented as percent infection relative to DMSO control (solid line).
46
47 The IC₅₀ and IC₉₀ values were calculated. Cell viability was determined in an
48
49 independent experiment in A549 or MDCK cells over a 24 or 48 hour period respective
50
51
52
53
54
55
56
57
58
59
60

1
2
3 to the infection conditions (dashed-line) and the CC_{50} and CC_{10} were calculated. Means
4
5 of three replicates \pm SD are shown.
6
7
8
9

10 **Figure 8. S119 analog, S119-8, synergizes with oseltamivir.** Isobolograms showing the
11 effect of fixed ratio combinations of S119-8 and (a) nucleozin or (b) oseltamivir. Each
12 circle represents the IC_{90} for the fixed ratio of the two inhibitors, while the diamonds
13 indicate the IC_{90} of each compound alone and the line connecting them is the isobole.
14
15
16
17
18
19
20
21
22
23
24
25
26
27
28
29
30
31
32
33
34
35
36
37
38
39
40
41
42
43
44
45
46
47
48
49
50
51
52
53
54
55
56
57
58
59
60

Circles underneath the isobole indicate a synergistic relationship, while circles above the isobole show antagonism between the compounds.

Table 1. S119 analogs have increased breadth of inhibition. Analogs of S119 were chemically synthesized and screened for antiviral activity against A/Puerto Rico/8/1934 (H1N1) and A/Vietnam/1203/2004 (H5N1-Halo) viruses which express GFP from the NS segment. GFP signal was detected by laser scanning cytometry and infectivity determined by GFP signal over counterstain of total cells.

Name	Structure	PR8	H5N1
		IC_{50} (μ M)	IC_{50} (μ M)

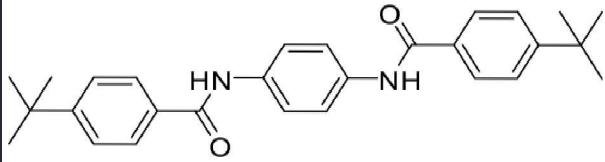
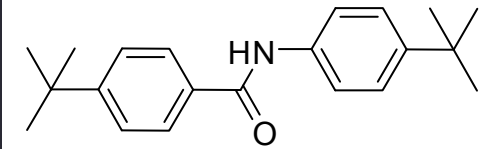
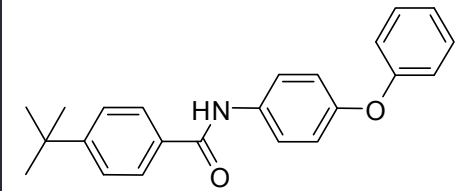
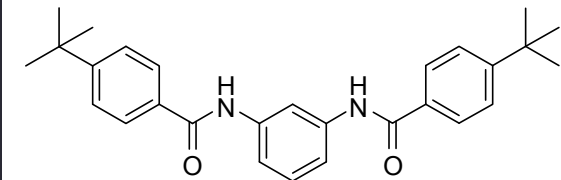
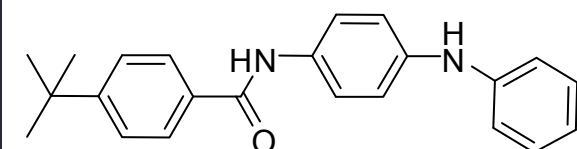
S119		>50	>50
S119-2		13.93	44.51
S119-3		11.41	17.37
S119-6		>50	>50
S119-8		6.05	8.42

Table 2. S119-8 shows increased breadth of activity against multiple influenza A and B viruses. S119 and S119-8 were tested against a number of influenza A and B viruses. Average IC_{50} and CC_{50} values of triplicate experiments are presented. Each strain indicated with a * was quantified using NP-staining of infected cells 24 hours post infection and signal was detected using the Celigo Imaging Cytometer (Nexcelcom Biosciences, Lawrence, MA). Infectivity was determined by NP signal over DAPI

counterstain of total cells. Otherwise, infections were quantified by standard plaque assay of supernatants from infected cells at 24 hours post infection.

Influenza virus	S119	S119-8	S119-8	Subtype/lineage	Cell Line
	IC ₅₀ (μ M)	IC ₅₀ (μ M)	CC ₅₀ (μ M)		
A/WSN/1933	0.02	1.43	>50	H1N1	A549
A/California/04/2009	27.43	5.32	>50	H1N1	A549
A/Puerto Rico/8/1934*	>50	6.05	>50	H1N1	A549
A/Brisbane/59/2007-S*	>50	6.68	40.66	H1N1	A549
A/Brisbane/59/2007-R*	>50	3.85	40.66	H1N1	A549
A/Panama/2007/1999	>50	6.43	>50	H3N2	A549
A/Wyoming/03/2003*	>50	11.53	40.66	H3N2	A549
A/Vietnam/1203/2004	>50	7.94	>50	H5N1	A549
B/Yamagata/16/1988	>50	2.08	>50	Yamagata	MDCK
B/Brisbane/60/2008*	>50	15.153	>50	Victoria	MDCK

Figure 1.

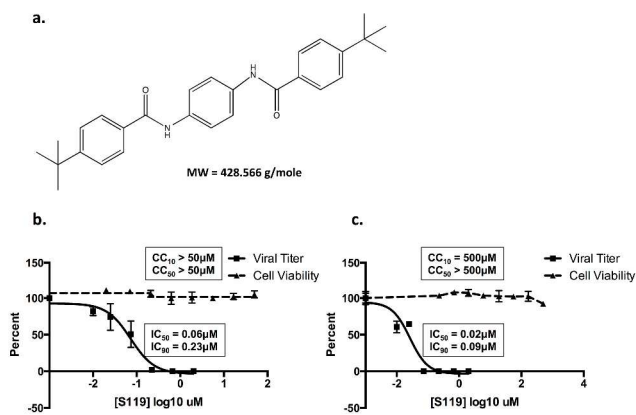


Figure 2.

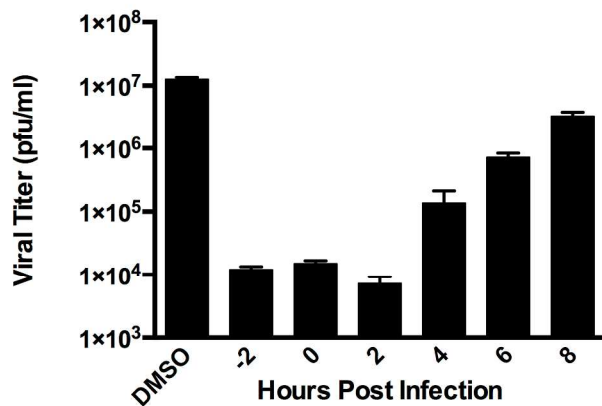


Figure 3.

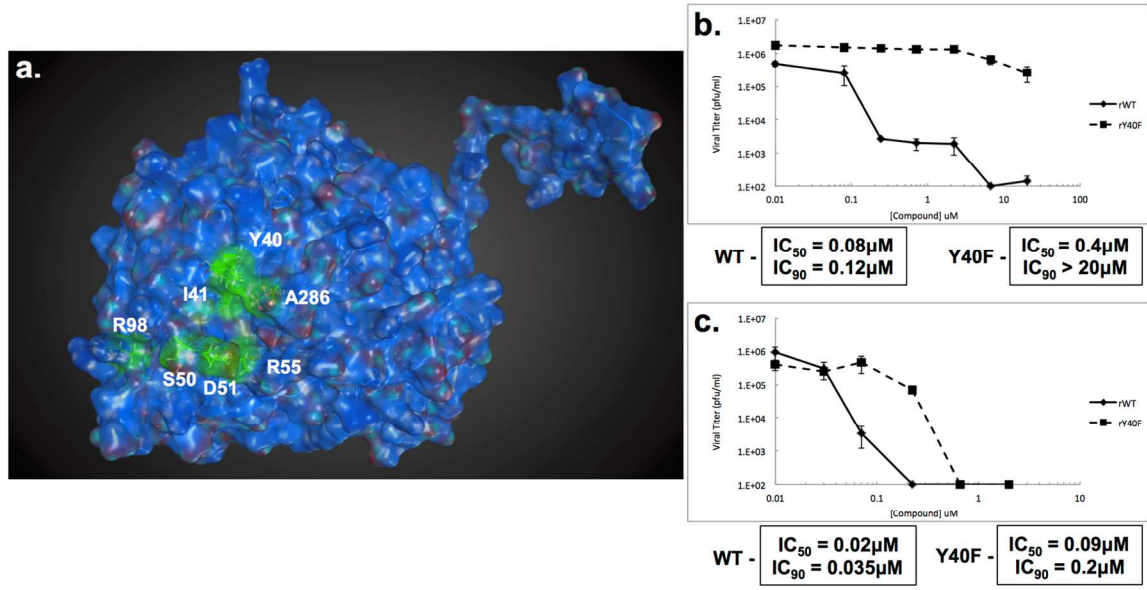


Figure 4.

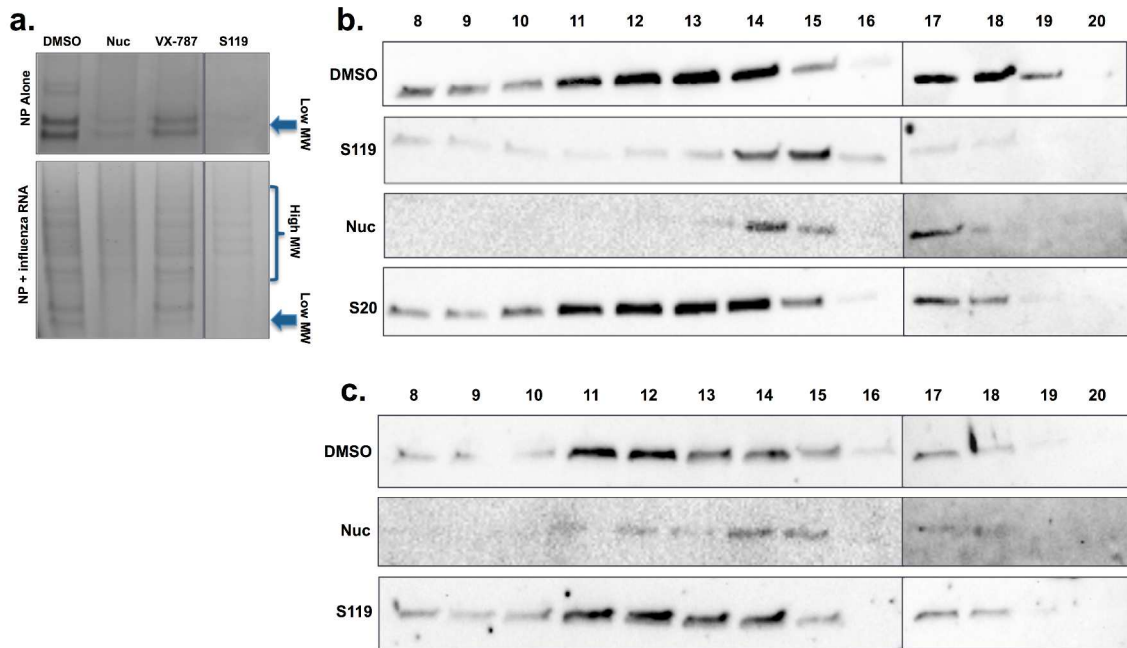


Figure 5.

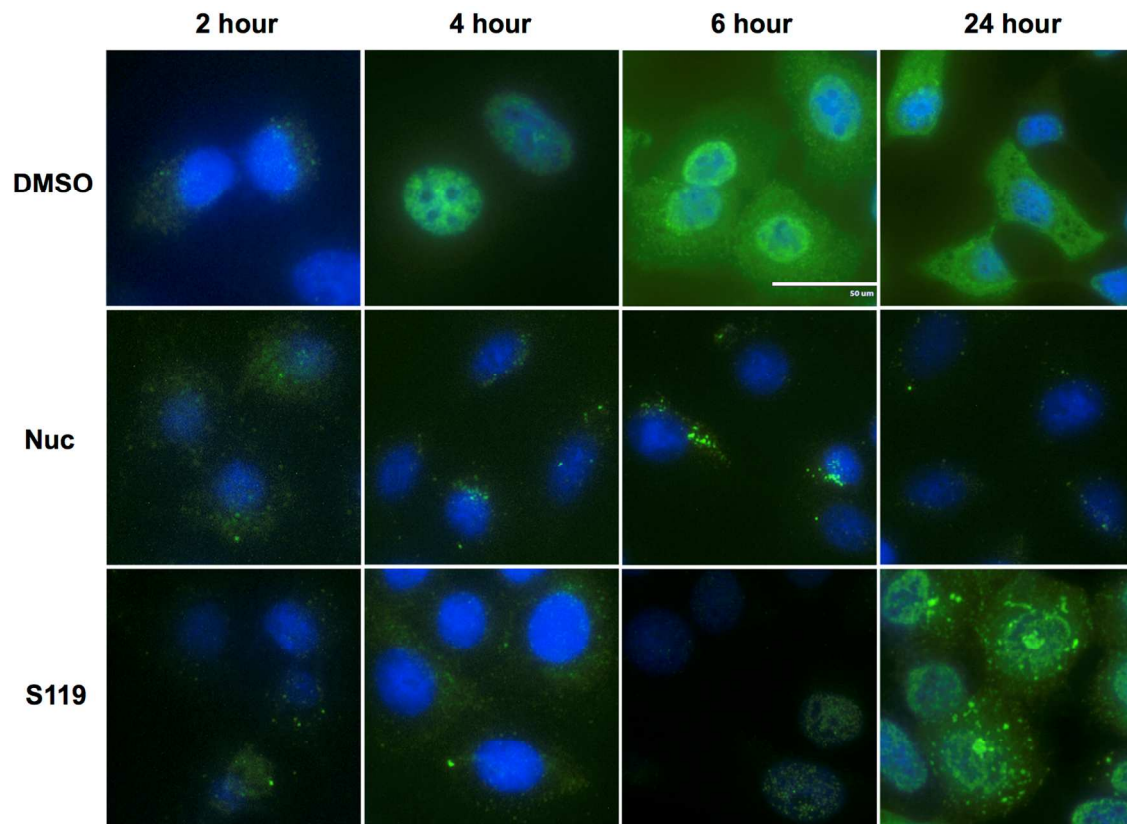


Figure 6.

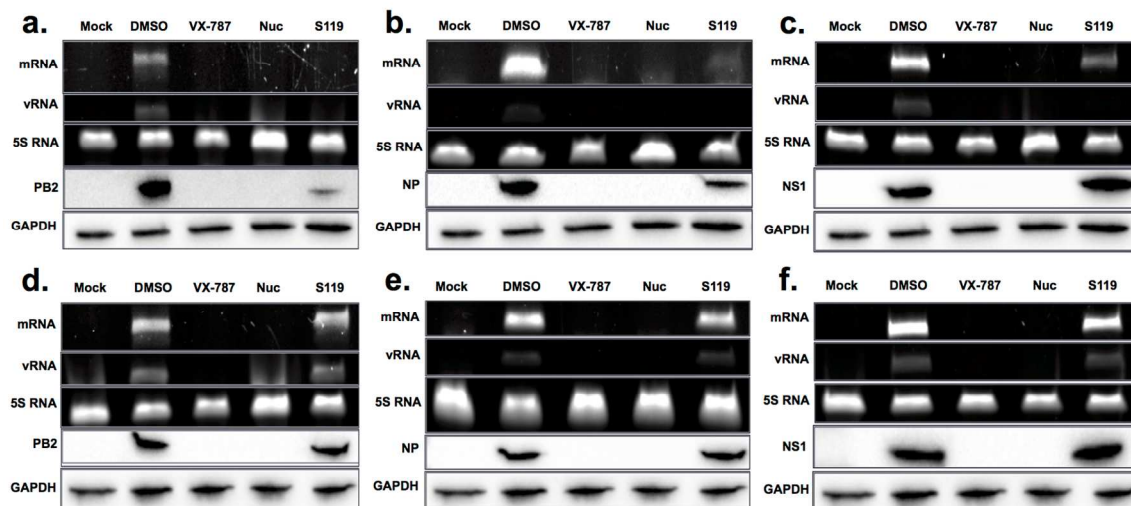


Figure 7.

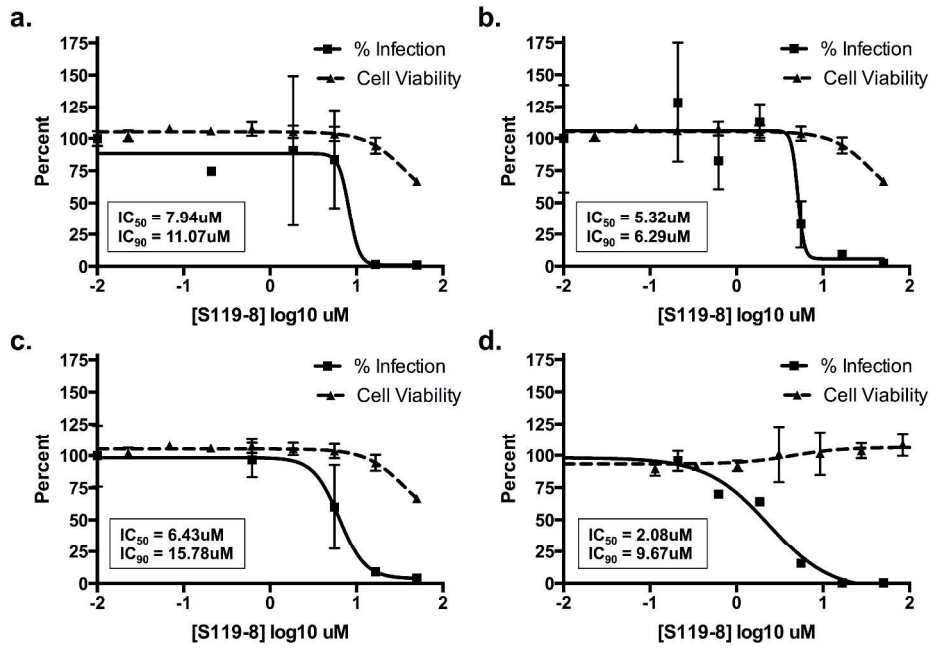
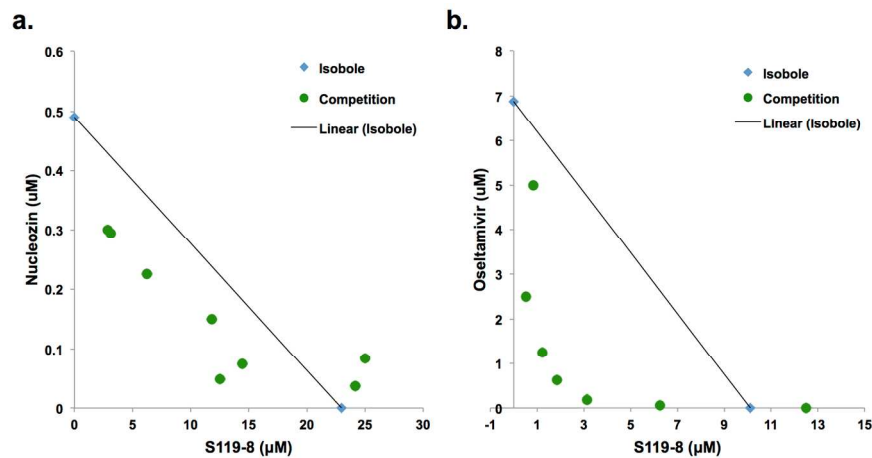


Figure 8.



1
2
3
4
5 **For Table of Contents only**
6

7
8 **Abstract Graphic**
9

